EUCLIPSE

EU Cloud Intercomparison, Process Study & Evaluation Project

Grant agreement no. 244067

Deliverable D2.7. Report on the identification of the processes or cloud types most responsible for climate change cloud feedbacks and precipitation responses.

Delivery date: 36 months

EUCLIPSE WP2 Deliverable D2.7:

Report on the identification of the processes or cloud types most responsible for climate change cloud feedbacks and precipitation responses.

Main contributors to this report:
Mark J. Webb (MetOffice/Hadley-Centre, UK), Sandrine Bony (LMD/IPSL, France), Daniel Klocke (ECMWF, UK), Gilles Bellon (CNRM, France) and Solange Fermepin (LMD/IPSL, France).

WP2 coordinator:
Sandrine Bony (CNRS/LMD/IPSL)

January 2013 (Month 36)

WP2 is focused on the analysis and the evaluation of climate simulations from CMIP5 (the 5th Phase of the Coupled Models Intercomparison Project). An important component of WP2 is the analysis of the climate response to anthropogenic perturbations, especially the changes in temperature, clouds and precipitation induced by the increase of greenhouse gases in the atmosphere. This deliverable reports on the identification of the processes or cloud types most responsible for the spreads of cloud feedbacks and precipitation projections in climate change experiments.

In collaboration with other workpackages (WP3 and WP4), the on-going EUCLIPSE research now aims at interpreting physically the reasons why these processes or cloud types differ amongst models and thus contribute to the spread of climate projections.

1 Decomposition of the inter-model spread in cloud feedback and cloud adjustment into contributions from areas dominated by different cloud types.

The cloud feedback classification method of Webb et al (2006) is used to decompose the inter-model spread in cloud feedback and cloud adjustment in the CMIP5/CFMIP-2 experiments into contributions from areas dominated by different types of clouds. Webb et al (2006) found that in CMIP3/CFMIP-1 mixed-layer slab mode experiments, regions where shortwave cloud feedbacks were stronger than the longwave cloud feedbacks were dominated by changes in low and mid-level clouds. They also found that these areas contributed more to the variance in global cloud feedback across these models than regions dominated other cloud types. Here we confirm that the latter conclusion continues to apply in the CMIP5/CFMIP-2 experiments with the current generation of models, and find that this applies not only to cloud feedbacks but also to cloud adjustments.

1.1 Introduction

Webb et al (2006) (hereafter W06) devised a classification system for local cloud feedbacks in climate models based on the relative strengths of their longwave and shortwave cloud feedback components (Figure 1). They assessed this classification method using outputs from the ISCCP simulator (Klein and Jakob, 1999, Webb et al, 2001) in nine CFMIP-1 slab model experiments, run to equilibrium following an instantaneous doubling of CO2 concentration. Regions where shortwave cloud feedbacks were stronger than longwave cloud feedbacks were found to be dominated by changes in low topped clouds, with mid-level topped clouds also making a smaller contribution. Conversely,

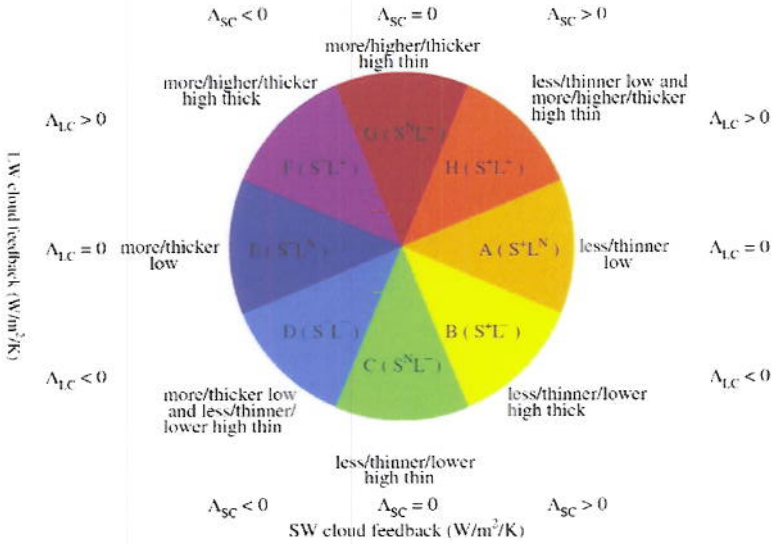

Figure 1: Cloud feedback classification from Webb et al (2006). Local values of the shortwave and longwave cloud feedback terms Λ_{SC} and Λ_{LC} are classified in a two-dimensional space with Λ_{SC} in the X dimension and Λ_{LC} in the Y dimension. Classes A(S^+L^N: orange) and E(S^-L^N: dark blue) contain cases where shortwave cloud feedbacks are stronger than relatively neutral longwave cloud feedbacks. Classes C(S^NL^-: green) and G(S^NL^+: dark red) contain cases where values of Λ_{SC} are relatively neutral compared with those of Λ_{LC}. Classes B(S^+L^-: yellow) and F(S^-L^+: purple) capture cases where Λ_{SC} and Λ_{LC} tend to oppose each other, while Classes D(S^-L^-: light blue) and H(S^+L^+:red) contain cases where Λ_{SC} and Λ_{LC} are of comparable size and the same sign. The cloud changes which dominate these classes in the CFMIP-1 models are also indicated.

regions where longwave cloud feedbacks were stronger than shortwave feedbacks, or longwave and shortwave cloud feedbacks approximately cancelled, were found to be dominated by changes in optically thinner and optically thicker high-topped clouds respectively. In some limited regions, longwave and shortwave cloud feedbacks were found to take the same sign. This behaviour was found to be associated with opposing changes in clouds at different levels – for example increases in thin cirrus accompanied by reductions in low level clouds. Regions with strong surface albedo feedbacks were placed in a separate feedback class, but found to be dominated by increases in low-level clouds. W06 also decomposed the inter-model variance in global cloud feedback across the CFMIP-1 slab model ensemble into contributions from these cloud feedback classes. The feedback classes dominated by changes in low-top clouds were found to explain 59% of this variance, compared to 33% for those dominated by high-top clouds, and 8% from the remaining "mixed" classes.

Subsequently, Soden and Vecchi (2011) applied this cloud feedback classification method to cloud feedback estimates from twelve CMIP3 coupled models subject to 1% per year increases in CO2 concentration. They diagnosed cloud feedbacks using the radiative kernel technique of Soden and Held (2006), which provides an estimate of the cloud feedback based on changes in cloud properties while excluding the effects of cloud masking. This was in contrast to the "Cloud Radiative Effect" method used in W06 and many earlier studies, which includes cloud masking effects (see Soden et al, 2004). Despite these differences, Soden and Vecchi also found the low-cloud feedback classes

made the largest contribution to the inter-model differences in cloud feedback, explaining roughly three quarters of the range. More recently, Zelinka et al (2012a) diagnosed cloud feedbacks from the CFMIP-1 models using a 'cloud radiative kernel' technique based in ISCCP simulator outputs, which allowed them to be decomposed into contributions from low, mid-top and high top clouds, as well as clouds with differing optical depths. Their results suggested a more important role for mid-level topped clouds than is apparent using the W06 feedback classification method, which does not separate the contributions from low and mid-level topped clouds.

A relatively new development in this area has been the finding that clouds can respond to changes in tropospheric and land surface temperatures which occur shortly after CO2 is increased, on much faster timescales than those mediated by the ocean response (Gregory and Webb (2008), Andrews and Forster (2008), Dong et al 2009)). Such rapid cloud adjustments have a radiative impact which can be considered part of the CO2 forcing. Inter-model differences in feedbacks explain considerably more of the inter-model spread in climate sensitivity than those in CO2 forcing (W06, Dufresne and Bony 2008), even when cloud adjustments are included in the CO2 forcing estimate (Webb et al 2012, Andrews et al 2012). Cloud feedback contributes four times as much as cloud adjustment to the range in climate sensitivity in the CMIP3/AR4 slab models (Webb et al 2012).

Zelinka et al (submitted) use their cloud radiative kernel technique to examine cloud adjustments and feedbacks in five CMIP5 model versions, but the number of models for which ISCCP simulator data is currently available is too small to draw robust conclusions about inter-model spread in cloud feedback. Although the Zelinka et al method is in some ways preferable to the W06 cloud feedback classification method, the latter has the advantage that it can be applied to all models, whether or not ISCCP simulator outputs are present. For this reason we consider it informative to repeat the W06 decomposition of the global cloud feedbacks and cloud adjustments in the CMIP5/CFMIP-2 presently available.

The CMIP5/CFMIP-2 experimental design (Bony et al (2011), Taylor et al 2011)) includes a number of atmosphere-only experiments which are relatively inexpensive compared to AOGCM experiments, and contain a wealth of additional process diagnostics designed to support investigation of the physical mechanisms underlying cloud feedbacks and adjustments. These are based on a control AMIP experiment forced with observed SSTs. Two SST perturbation experiments are included, where the AMIP SSTs are increased uniformly by 4K (amip4K) and a patterned SST perturbation scaled to 4K, based on a composite SST response from coupled models in CMIP3 (amipFuture). A CO2 quadrupling experiment with fixed AMIP SSTs (amip4xCO2) is also included for the analysis of cloud adjustments (following Hansen 2005). Here we apply the cloud feedback W06 decomposition method to these experiments to see the extent to which cloud feedbacks and adjustments are dominated by the responses of low clouds. We do this not only to see whether or not low clouds continue to dominate inter-model differences in cloud feedbacks in CMIP5/CFMIP-2, but also to establish the extent to which the CFMIP-2 atmosphere only experiments can capture this behaviour, and so provide a test-bed for further investigations.

1.2 Results and Discussion

Figure 2 shows the contributions of the W06 feedback classes to the inter-model spread in cloud feedback and adjusted CO2 forcing in the CFMIP-1 experiments from W06, and CMIP5/CFMIP-2 experiments listed in Table 1. The variance in the total feedback and adjusted forcing across each ensemble is decomposed into contributions from the global cloud feedbacks and cloud adjustments, and the contributions to these from the different feedback classes using an additive variance decomposition (see W06 for details). Figure 2(a) summarises the results from W06 from CFMIP-1, showing that the cloud feedback explains 66% of the total feedback variance, and that 59% of this is due to

AGCM	AMIP4	AMIP4xCO2	AmipFuture	AmipFuture Cloud Masking	Amip4K	Amip4K Cloud Masking
CNRM-CM5	X	X	X		X	X
CanAM4	X	X	X	X	X	X
FGOALS-G2	X				X	
HadGEM2-A	X	X	X	X	X	X
IPSL-CM5A-LR	X	X	X		X	
MIROC5	X	X	X	X	X	X
MPI-ESM-LR	X	X	X	X	X	X
MPI-ESM-MR	X	X	X		X	
MRI-CGCM3	X	X	X		X	
NorESM1-M	X	X				
Nb of models	10	9	8	4	9	5

Table 1: Data available from CMIP5/CFMIP-2 GCM experiments.

the low-top dominated classes A,E and I. The high-top dominated classes (C, G, B and F) explain 33% of the cloud feedback variance, while the mixed classes explain 8%. As discussed above, the calculations in W06 did not separate the effects of cloud masking and cloud changes, or the effects of cloud adjustment and cloud feedback. We have made allowances for both of these in our analysis of the CFMIP-2 data, as follows.

For the cloud adjustments, we calculated the annual mean climatology of the change in the net CRE between the amip and amip4xCO2 experiments listed in Table 1. We then made allowance for the cloud masking effect by removing the longwave cloud masking diagnosed for CO2 quadrupling from HadGEM2-A. A more satisfactory approach in future might be to remove cloud masking diagnosed from each model individually, but the necessary diagnostics are not currently available from all of the models. Figure 2(b) shows that cloud adjustments explain 46% of the variance in the adjusted forcing, and that 62% of the cloud contribution is due to the low-top dominated classes A and E. (Class I is not calculated for cloud adjustment as surface albedo does not change appreciably.) The high-top cloud dominated classes contribute 24%, while the mixed classes contribute 14%. Note that cloud adjustments explain a smaller fraction of the inter-model variance in adjusted CO2 forcing than the fraction of total feedback variance explained by cloud feedback.

For the amip4K and amipFuture SST perturbation experiments, we calculated the change in the annual mean climatology of the net CRE relative to the amip control, and removed an estimate of the longwave cloud masking effect calculated using the cloud radiative kernel method, kindly provided by Mark Zelinka. This was done by removing the ensemble mean longwave cloud masking from the models which have ISCCP simulator data available (see Table 1). As in W06 we deal with the shortwave cloud masking effect by separating areas with substantial surface albedo feedbacks into their own class (class I). These contribute very little to the inter-model spread in the cloud feedback because sea ice concentrations are unperturbed in the amip4K and amipFuture experiments. In the amip4K experiments, 87% of the variance in the total feedback is explained by cloud feedback, and the classes dominated by low topped clouds (A, E and I) explain 68% of the cloud feedback contribution. The high-top classes explain 13%, while the mixed classes explain 19%.

In the case of the amipFuture experiments however, the low top classes explain 41%, compared to 25% for the high top classes and 34% for the mixed class. Although the low-top classes do still explain more of the cloud feedback variance than the high-top classes or the mixed classes in this case, they explain less than 50% of the total contribution from the cloud feedback, in contrast to the situation in the the CFMIP-1, amip4xCO2 and amip4K

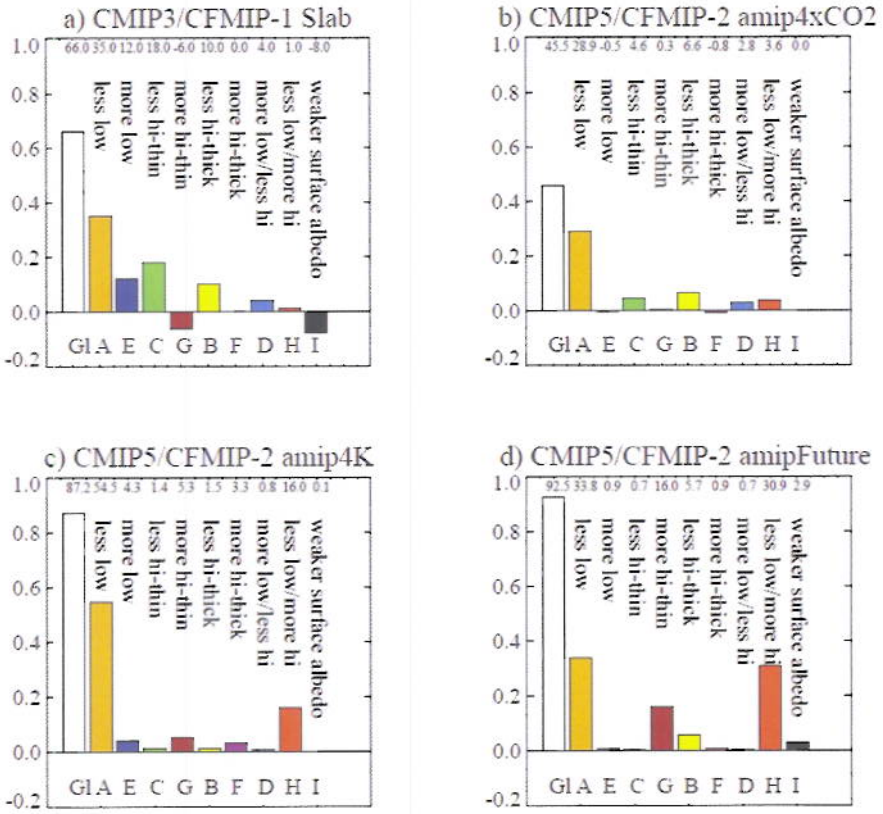

Figure 2: Contributions to inter-model spread in cloud feedbacks (a,c,d) and cloud adjustments (b) from the feedback classes defined in Figure 1. The white bars show the percentage of the variance in the total feedback and adjusted forcing across each ensemble due to global cloud feedback or adjustment. The coloured bars show the contributions from the individual feedback classes.

ensembles. The amipFuture ensemble has larger contributions from class G, which is associated with a positive feedback from thin cirrus clouds, and from class H which is associated with a positive longwave cloud feedback from thin cirrus combined with a positive shortwave feedback from low-level clouds. Examination of the individual models shows unusually large positive cloud feedbacks in these classes in IPSL-CM5-LR in the amipFuture experiment in the Eastern subtropical Pacific and Atlantic, which suggests a stronger sensitivity to the changing SST pattern in this particular model. This may be a consequence of the eastward shift of deep convection in the tropical Pacic noted by Vecchi and Soden (2007) being stronger in some models than others (Webb et al, 2012). The contribution from the mixed class H is due in approximately equal parts to inter-model differences the strength of the positive shortwave cloud feedback within this class (primarily due to low clouds) and those in the positive longwave cloud feedback (due to thin cirrus clouds) (not shown). If the shortwave and longwave contributions from the mixed classes are added to those from the low and high-top cloud dominated classes respectively, then the low cloud total contributes 59% to the variance of the cloud feedback, while high cloud total contributes 41%.

To give an indication of the relative contributions of different geographical regions to inter-model spread in cloud feedbacks and cloud adjustments, we show standard deviation maps in Figure 3. These are normalised to have global means equal to unity, to support a relative comparison of cloud adjustments and cloud feedbacks. The cloud feedbacks

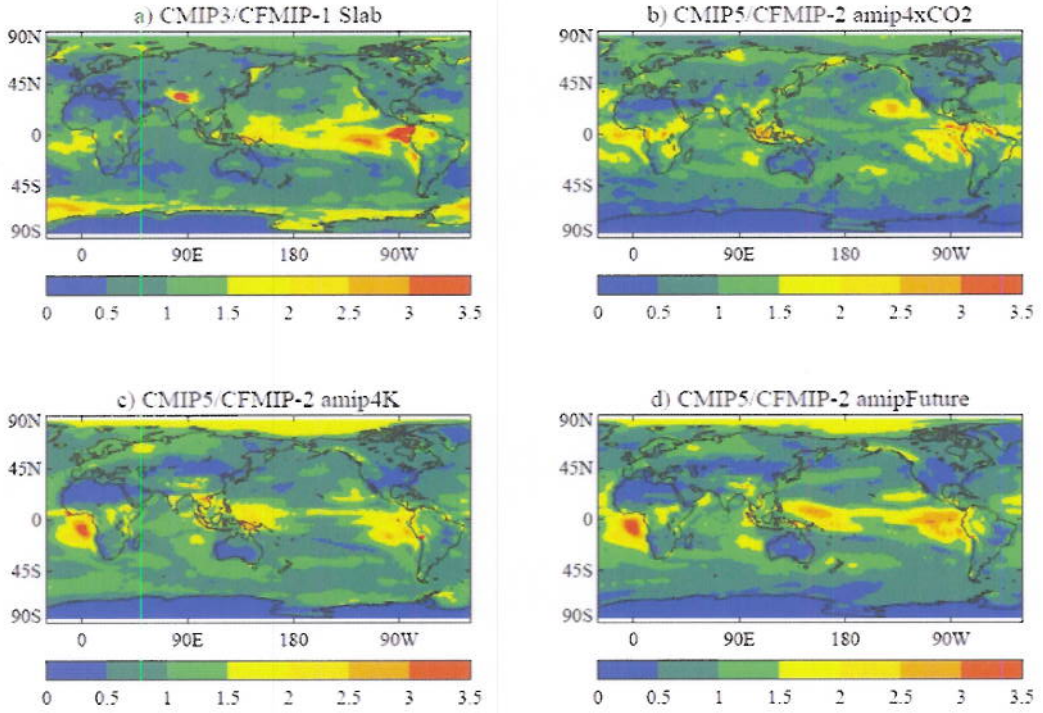

Figure 3: Relative contributions of cloud feedbacks (a, c and d) and cloud adjustments (b) from different parts of the globe. The maps show local standard deviations across each ensemble, normalised to the same global mean.

in the CFMIP-1, amip4K and amipFuture ensembles, and the cloud adjustments in the amip4xCO2 ensemble all show large standard deviations in the subtropical stratocumulus and trade cumulus regions, underscoring the dominant contribution of low clouds to inter-model spread in cloud feedback and cloud adjustment. Large standard deviations in cloud feedbacks are also seen in deep convective regions which may be indicative of shifts in deep convection which differ from model to model. The responses in subtropical areas are often strongly correlated with the global mean cloud feedback, but this is not the case for the deep convective regions (not shown). This may be a consequence of the deep convective feedbacks operating over a much smaller area than the low cloud feedbacks.

2 Analysis of the spread of tropical precipitation projections

In CMIP5 like in CMIP3, precipitation projections from climate models exhibit a large spread at the regional scale, especially in the tropics. In Deliverable 2.6, we presented an analysis framework of regional precipitation projections decomposing the precipitation change into dynamic and thermodynamic components, and into fast and slow responses. This analysis framework was used to interpret the robust multi-model mean pattern of precipitation changes in a climate change scenario assuming no mitigation. Here, we use this framework to analyze the inter-model spread of tropical precipitation projections. We show that most (about 70%) of this spread comes from the dynamic

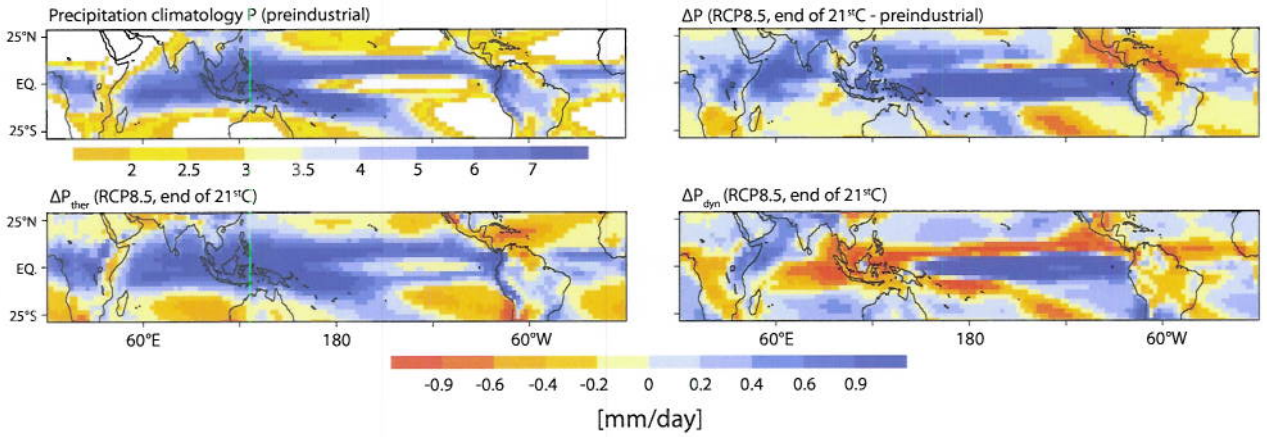

Figure 4: Multi-model mean projection of tropical precipitation changes at the end of the 21st century. The upper left panel shows the climatological multi-model mean annual precipitation (in mm/day) simulated by sixteen CMIP5 climate models (including models from four EUCLIPSE modeling groups) in the pre-industrial climate. Other panels show the multi-model mean change in annual precipitation projected by the same models (upper right) and its decomposition ($\Delta P = \Delta P_{\rm ther} + \Delta P_{\rm dyn}$) into thermodynamic ($\Delta P_{\rm ther}$) and dynamic ($P_{\rm dyn}$) components at the end of the 21st century in a climate change scenario without mitigation (RCP8.5).

component, and that inter-model differences in the thermodynamic component are correlated with differences in the present-day climatology of precipitation. These results guide our on-going efforts to better interpret uncertainties in regional precipitation projections.

2.1 Spread of precipitation projections

We interpret the response of tropical precipitation by dividing it into two components : a dynamic one due to circulation changes, and one independent of these. Using the vertically-averaged large-scale vertical (pressure) air velocity $\bar{\omega}$ as a proxy for large-scale atmospheric motions, we diagnose the dynamic component ($\Delta P_{\rm dyn}$) as the contribution to ΔP from changes in $\bar{\omega}$. The remaining change is referred to as the thermodynamic component, $\Delta P_{\rm ther}$, i.e., $\Delta P = \Delta P_{\rm dyn} + \Delta P_{\rm ther}$ (Bony et al. 2012). The multi-model mean ΔP, $\Delta P_{\rm ther}$ and $\Delta P_{\rm dyn}$ are shown on Figure 4.

$\Delta P_{\rm ther}$ exhibits a "wet get wetter, dry get drier" regional pattern**?**. This is primarily explained by the increase of atmospheric water vapour with temperature (following the Clausius-Clapeyron thermodynamic relationship), and the associated increase of moisture convergence in the moist, rising branches of the present-day tropical circulation and moisture divergence from the dry, subsidence regions. This pattern is thus closely related to the climatological distribution of precipitation. In contrast, circulation changes lead to a more complex pattern of precipitation changes ($\Delta P_{\rm dyn}$).

As explained in Deliverable 2.6., a large part of the long-term circulation response (and thus the dynamic component of the precipitation response) to increased greenhouse gases does not depend on global warming but results from the fast and direct effect of CO_2 on the large-scale atmospheric circulation (the reduced radiative cooling of the troposphere associated with increased CO_2 weakens the upward and downward large-scale vertical motions and the strength of the overturning circulation). This effect, which depends on very fast processes, is not primarily mediated by surface warming nor by land-sea contrasts.

Figure 5 shows the inter-model spread across CMIP5 models of regional precipitation projections in a climate change scenario without mitigation (RCP8.5). The spread is maximum over tropical oceans and the maritime conti-

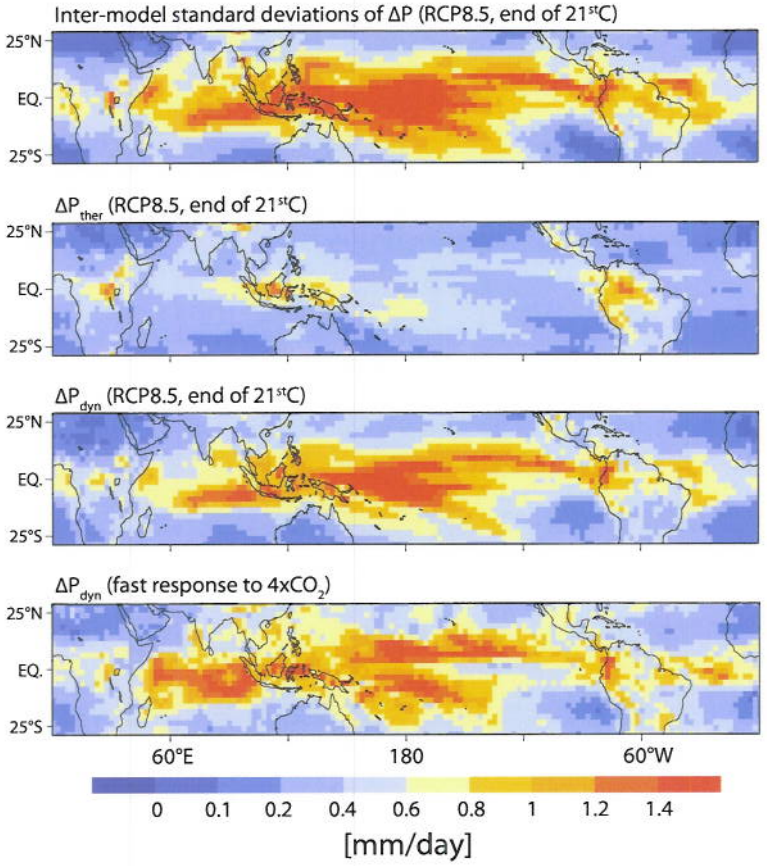

Figure 5: Inter-model spread of regional precipitation projections in the tropics. The upper panel shows the spread (inter-model standard deviation, in mm.day^{-1}) of precipitation changes projected by 14 CMIP5 OAGCMs in the RCP8.5 scenario at the end of the 21st century. The two middle panels show the spread of the thermodynamic and dynamic components of precipitation changes in the same models and the same scenario. The bottom panel shows the spread of the fast dynamic component of precipitation changes inferred from the first simulated year of abrupt4xCO2 experiments. The tropical-mean standard deviations of the different panels from top to bottom are: 0.69, 0.35, 0.58 and 0.63 mm.day^{-1}.

nent, with secondary maxima over South America and central Africa. Over ocean, most of the spread results from inter-model differences in the dynamic component. Over land, the contributions of the dynamic and thermodynamic components is more equal. Over the tropics as a whole, about 70% of the regional spread comes from the dynamic component.

2.2 Early analysis of the spread

The sign and the amplitude of the thermodynamic component ΔP_{ther} is closely related to the climatological distribution of precipitation (Bony et al. 2012). This result, which is true for any individual model, suggests that inter-model differences in the simulation of the present-day (or pre-industrial) precipitation pattern likely translate into differences in the thermodynamic component of precipitation projections. It is verified by Figure 6, which shows that the regional pattern of $\Delta P_{\text{ther}}/\Delta T_s$ is highly correlated to the climatological pattern of precipitation.

The dynamic component, which explains most of the regional spread of precipitation projections, deserves a more detailed analysis. As a first step, we examined how much inter-model differences in the long-term dynamic component could be related to differences in the fast response of the circulation to anthropogenic forcings. Figure 5

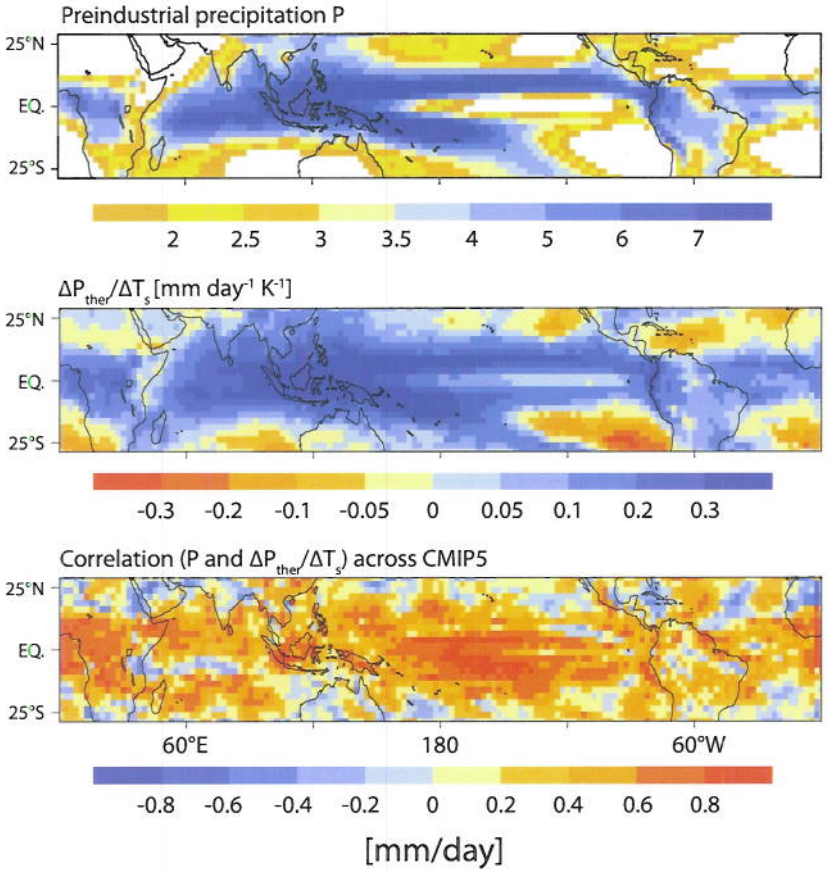

Figure 6: Correlation between precipitation climatology and the thermodynamic component of precipitation changes The upper panel shows the multi-model mean pattern of annual precipitation (in mm/day) derived from 16 CMIP5 OAGCMs in the pre-industrial climate (piControl). The middle panel shows the multi-model mean pattern of the thermodynamic component of precipitation changes normalised by the local surface warming ($\Delta P_{\rm ther}/\Delta T_s$, expressed in mm/day/K) inferred from the same models in abrupt4xCO2 experiments. The bottom panel shows the correlation (across 16 CMIP5 models) between the precipitation climatology and the thermodynamic component predicted by individual models.

shows that the fast dynamic component of precipitation changes is significant in regions where the spread of the long-term dynamic component is the largest.

Figure 7 quantifies the correlation across CMIP5 models between the fast and long-term dynamical patterns of $\Delta P_{\rm dyn}$. Over land areas (e.g. over Africa), the signs of the fast and long-term dynamic components are often opposite. This is consistent with the antagonist effects of CO2 and temperature (local surface warming and transient land-sea contrasts) on large-scale rising motions over land (Bony et al. 2012). Over many areas of tropical oceans, but also over part of Amazonia and of the Sahel, the fast Pdyn correlates quite strongly with the long-term component (correlation across models > 0.6 or 0.8). Gaining confidence in the pattern of the fast dynamic component may thus be a way to gain confidence in a key component of long-term precipitation projections.

Our on-going research aims at understanding further the origin of the spread of $\Delta P_{\rm dyn}$, especially the physical mechanisms underlying the responses of the atmospheric circulation to greenhouse gases and temperature. Results will be reported in deliverable D2.8.

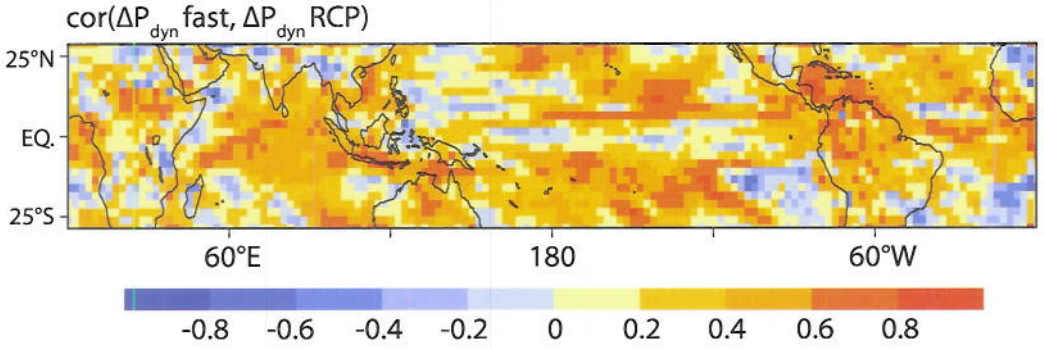

Figure 7: Inter-model correlation between fast and long-term dynamic components of precipitation changes. The figure shows the linear correlation coefficient (computed across 14 CMIP5 models) between the fast dynamic response of precipitation to increased CO_2 ($\Delta P_{\rm dyn}$ fast, inferred from the first year of abrupt4xCO2 experiments) and the long-term dynamic response of precipitation ($\Delta P_{\rm dyn}$ RCP, estimated from RCP8.5 experiments at the end of the 21$^{\rm st}$ century).

2.3 References

Andrews, T., and P.M. Forster (2008), CO2 forcing induces semi-direct effects with consequences for climate feedback interpretations. Geophys. Res. Lett., 35, L04802, doi:10.1029/2007GL032273.

Andrews, T., J. M. Gregory, M. J. Webb, and K. E. Taylor (2012), Forcing, feedbacks and climate sensitivity in CMIP5 coupled atmosphere-ocean climate models, Geophys. Res. Lett., 39, L09712, doi:10.1029/2012GL051607.

Boer, G.J. and B. Yu (2003), Dynamical aspects of climate sensitivity. Geophys. Res. Lett., 30(3), 1135.

Bony, S., et al. (2011), CFMIP: Towards a better evaluation and understanding of clouds and cloud feedbacks in CMIP5 models. Clivar Exchanges, 56, 16, 2.

Bony, S., Bellon, G., Klocke, D., Sherwood, S., Fermepin, S., and S. Denvil. Direct effect of carbon dioxide on future tropical atmospheric circulation and regional precipitation. *Nature Geoscience*, in revision.

Dufresne, Jean-Louis, Sandrine Bony (2008), An Assessment of the Primary Sources of Spread of Global Warming Estimates from Coupled Atmosphere-Ocean Models.J. Climate,21, 5135–5144.

Dong, Buwen, Jonathan M. Gregory, Rowan T. Sutton, 2009: Understanding Land-Sea Warming Contrast in Response to Increasing Greenhouse Gases. Part I: Transient Adjustment.J. Climate,22, 3079–3097.

Gregory, J.M. and M.J. Webb (2008), Tropospheric adjustment induces a cloud component in CO2 forcing. J. Climate, 21, 58-71, doi:10.1175/2007JCLI1834.1.

Hansen, J., et al. (2005), Efficacy of climate forcings. J. Geophys. Res., 110, D18104, doi:10.1029/2005JD005776.

Klein, S. A. and Jakob, C. (1999), Validation and sensitivities of frontal clouds simulated by the ECMWF model. Mon. Weather Rev., 10, 2514-2531

Soden, B. J., A. J. Broccoli, and R. S. Hemler, (2004), On the use of cloud forcing to estimate cloud feedback. J. Climate, 17, 36613665.

Soden, B.J., I.M. Held (2006), An Assessment of Climate Feedbacks in Coupled OceanAtmosphere Models. J. Climate, 19, 33543360.

Soden, B. J., and G. A. Vecchi (2011), The vertical distribution of cloud feedback in coupled ocean-atmosphere models, Geophys. Res. Lett., 38, L12704, doi:10.1029/2011GL047632.

Taylor, K.E., R.J. Stouffer and G.A. Meehl (2011), An overview of CMIP5 and the experiment design. Bull. Amer. Meteor. Soc., doi:10.1175/BAMS-D-11-00094.1.

Vecchi, G.A., and B.J. Soden (2007), Global Warming and the Weakening of the Tropical Circulation. J. Climate,

20, 4316-4340.

Webb, M. and Senior, C. and Bony, S. and Morcrette, J. J. (2001), Combining ERBE and ISCCP data to assess clouds in the Hadley Centre, ECMWF and LMD atmospheric climate models. Clim. Dyn. 17 905-922.

Webb, M.J., et al. (2006), On the contribution of local feedback mechanisms to the range of climate sensitivity in two GCM ensembles, Clim. Dyn., 27, 17-38.

Webb, M. J. and Lambert, F. H. and Gregory, J. M. Origins of differences in climate sensitivity, forcing and feedback in climate models, (2012) Clim. Dyn. 10.1007/s00382-012-1336-x

Zelinka, M.D., S.A. Klein, and D.L. Hartmann, (2012), Computing and Partitioning Cloud Feedbacks Using Cloud Property Histograms. Part II: Attribution to Changes in Cloud Amount, Altitude, and Optical Depth. J. Climate, 25, 37363754. doi:10.1175/JCLI-D-11-00249.1.1

Zelinka, M.D., S.A. Klein, K.E. Taylor, T. Andrews, M.J. Webb, J.M. Gregory, and P.M. Forster, (2012b): Contributions of Different Cloud Types to Feedbacks and Rapid Adjustments in CMIP5. Submitted to J. Climate.

2.4 Acknowledgements

We are grateful to Mark Zelinka who provided cloud masking estimates for a subset of the CFMIP-2 models used in this work, and to Steven Sherwood and Jean-Louis Dufresne for insightful comments about our results. We acknowledge the World Climate Research Programme's Working Group on Coupled Modelling, which is responsible for CMIP, and we thank the climate modelling groups for producing and making available their model output. For CMIP the U.S. Department of Energy's Program for Climate Model Diagnosis and Intercomparison provides coordinating support and led development of software infrastructure in partnership with the Global Organization for Earth System Science Portals.